AIAA JOURNAL
Vol. 35, No. 5, May 1997

Nd:YAG Laser-Based Dual-Line Rayleigh Scattering System

M. V. Ötügen,* J. Kim,† and S. Popović‡
Polytechnic University, Brooklyn, New York 11201-3840

A dual-line detection Rayleigh scattering system for temperature and pressure diagnostics of gas flows is presented. The system, which uses two harmonics of an Nd:YAG laser simultaneously, is similar to an earlier version that utilized a copper-vapor laser. The dual-line detection method allows the determination and subsequent removal of surface-scattered background noise from the Rayleigh signal, improving the applicability of Rayleigh scattering to enclosed flows with high levels of laser glare. The present system was tested in both a vacuum chamber and a heated turbulent air jet covering a range of gas pressures and temperatures and in the presence of various levels of background noise. The 532-nm second and the 266-nm fourth harmonics of the laser were used simultaneously to collect scattered signal. Comparison of results obtained by the present system to those of single-line Rayleigh scattering shows that the dual-line detection technique provides a substantial improvement in measurement accuracy. The new system can accurately measure gas temperature and pressure up to a point where the background noise-to-Rayleigh signal ratio is approximately 3 on the green line. The surface scattering coefficient for the 266-nm uv line was found to be half that of the 532-nm green line, making the Rayleigh signal-to-background noise ratio of the uv line 30 times higher than that of the green line.

Nomenclature

C	= calibration constant for optical system
C'	= surface scattering constant
d	= inner jet diameter at exit
E_B	= background energy
E_L	= incident laser energy
E_R	= Rayleigh scattered energy
E_T	= total detected energy
P	= gas pressure
r	= radial jet coordinate
T	= mean gas temperature
T'	= rms of fluctuating temperature
x	= axial distance from jet exit
β	= surface scattering ratio, C_1'/C_2'
ΔC	= uncertainty in C
ΔP	= uncertainty in pressure
κ	= Boltzmann's constant
λ	= laser wavelength
σ	= Rayleigh scattering differential cross section

Subscripts

c	= coflow
j	= jet
1	= 532-nm line
2	= 266-nm line

Introduction

RAYLEIGH scattering is an attractive technique for the nonintrusive measurement of gas flow properties such as density, temperature, mixture concentration and, in the case of high-speed flows, velocity. Compared to other molecular scattering methods, it is relatively easy to set up and the interpretation of the data is straightforward. It can provide space- and time-resolved information about the flowfield. The technique has been used in both reacting and nonreacting flows, in most cases with considerable success. For example, Rayleigh scattering was used to measure density and temperature in external, premixed jet flames.[1–4] In nonreacting flows, it has been used to measure concentration in binary gas jets[5–8] and temperature in heated jets.[9] In all these experiments, the intensity of the Rayleigh scattered light is measured to determine both the density (or concentration) and the temperature of the interrogated gas. More recently, Rayleigh scattering has been applied to high-speed flows as a velocity probe.[10–13] In this application, a narrow-line laser is used and the central Doppler shift of the Rayleigh scattered light is related to the gas velocity. The spectral characteristics of the Rayleigh signal can also be used to determine gas temperature and pressure.[14]

When Rayleigh scattering has been applied to external flows, results have generally been more successful than when the method has been attempted in enclosed environments. In external flows, it is relatively easy to control the surface scattered laser light (or glare), which can potentially contaminate the Rayleigh scattering. In internal flows, surface-scattered laser light is stronger due to multiple reflections from test section walls and optical windows and, therefore, can generate background levels high enough to contaminate the Rayleigh signal. In particular, if the Rayleigh scattered light is collected at near-forward or near-backward angles, this background noise can completely overwhelm the signal. When the flow velocity is high enough to generate a significant Doppler shift in the Rayleigh scattering spectra, the unshifted background noise can be eliminated by using sharp-edged gas molecule absorption filters. For example, iodine molecular filters have been used in conjunction with Nd:YAG lasers for Rayleigh scattering measurements in supersonic wind tunnels.[12,14] However, in most low-speed flows, such as those in combustors, the Rayleigh scattered light from the gas molecules and surface scattered background noise have approximately the same central frequency and, therefore, such filtering techniques cannot be used.

Ötügen et al.[15] recently presented a dual-line detection Rayleigh scattering (DLDR) technique to address the problem of signal contamination by surface-scattered laser light. They used the two lines of a copper-vapor laser with a single set of transmitting and collecting optics to capture and analyze signal from both the 578- yellow and 510-nm green lines. In this technique, a two-equation system is formed with the Rayleigh scattering signal and background noise as the two independent variables, thus enabling determination of background noise due to laser glare, which can then be removed from the Rayleigh signal. Using this copper-vapor laser-based system, they obtained accurate temperature measurements even when the background noise was twice that of the Rayleigh signal.

Received June 29, 1996; revision received Jan. 13, 1997; accepted for publication Jan. 17, 1997.

*Associate Professor, Mechanical, Aerospace, and Manufacturing Engineering. Senior Member AIAA.

†Graduate Student, Mechanical, Aerospace, and Manufacturing Engineering.

‡Research Scientist, Weber Research Institute.

Copper-vapor lasers, however, are limited in their applicability to Rayleigh scattering in that they offer relatively low-pulse energies compared to Nd:YAG lasers. The high-pulse energies of Nd:YAG lasers are better suited for time-resolved measurements and also provide better beam characteristics. In this report, an Nd:YAG laser-based DLDR system is presented. The system uses the 532-nm second and 266-nm fourth harmonics of the laser and, again, a single set of transmitting and collecting optics is used to form the optical probe and to gather scattered light from it. The system was calibrated and tested under several background noise levels using both a vacuum chamber and a heated air jet as the test environment. Finally, turbulent temperature measurements were made in a hot air jet and results were compared to those obtained by a fast-response thermistor in the same jet. An analysis was also carried out to estimate the uncertainty characteristics of the system. The single-shot measurement uncertainty determined from shot-noise statistics compared favorably with the statistics of the actual measurements.

Experimental System

Dual-Line Detection Technique

Because a detailed description of the DLDR method is provided in Ref. 15, only a brief description of the technique will be provided here. A single beam containing two lines of the laser is used in the DLDR technique. The Rayleigh scattered light from the probe volume is collected and collimated using a single lens. Subsequently, the signals from the two lines are separated using a dichroic splitter and sent to separate detectors providing a linear system of two equations with Rayleigh scattered light energy and background noise as two unknowns, both normalized with the laser energy at the appropriate line. The two equations are independent and lead to a unique solution because the wavelength dependence of Rayleigh scattered light and surface scattered light are different. Still, the greater the disparity is between the two wavelengths, the more robust the system. Therefore, the present system using the second and fourth harmonic lines of the Nd:YAG laser is superior to the earlier copper-vapor laser-based system, which used the 578- and 510-nm lines.[15]

Using the equation of state for a perfect gas, the system of equations for the DLDR system can be expressed as follows:

$$E_{T,1}/E_{L,1} = C_1[(\sigma_1 P/\kappa T) + \beta C'] \tag{1}$$

$$E_{T,2}/E_{L,2} = C_2[(\sigma_2 P/\kappa T) + C'] \tag{2}$$

In the present system, $\lambda_1 = 532$ nm and $\lambda_2 = 266$ nm. The system can be calibrated to determine C_1 and C_2, under known pressure and temperature conditions. C' represents the background level and β is the ratio of surface scattering at the two wavelengths, which is also determined through the calibration process. Through Eqs. (1) and (2) the system provides a direct measurement of pressure or temperature independent of the background noise. For example, if gas pressure is the quantity to be measured, the system yields

$$P = \left(\frac{E_{T,1}}{E_{L,1}}\frac{1}{C_1} - \frac{E_{T,2}}{E_{L,2}}\frac{\beta}{C_2}\right)\Big/\left(\frac{\sigma_1 - \beta\sigma_2}{\kappa T}\right) \tag{3}$$

along with

$$C' = \left(\frac{E_{T,2}}{E_{L,2}}\frac{\sigma_1}{C_2} - \frac{E_{T,1}}{E_{L,1}}\frac{\sigma_2}{C_1}\right)\Big/(\sigma_1 - \beta\sigma_2) \tag{4}$$

Equation (4) does not provide any information regarding the flow, but it serves the purpose of determining the reliability of a measurement. Although Eqs. (3) and (4) completely decouple pressure and background, there is a threshold value of C' for each system above which reliable measurements are not possible mainly due to the saturation of one or more of the electronic/optical components of the system. Once this threshold value of C' is determined through the initial calibration, it can be used as a flag against unreliable measurements.

Rayleigh Scattering System

The optical arrangement for the DLDR system is shown in Fig. 1. The output of the laser at the 1064-nm fundamental frequency is doubled through a harmonic generator to produce the 532-nm second harmonic. The residual infrared is removed from the 532-nm green line using a harmonic separator and directed into a beam dump. The green line is passed through a fourth harmonic generator where the frequency is again doubled to generate 266-nm uv line along with the residual 532-nm light. The green and the uv lines are polarized at 90 deg to each other. The half-wave plate before the fourth harmonic generator is rotated such that the polarization direction of the second and fourth harmonic lines are ±45 deg to the direction along which the Rayleigh scattered light is collected. Because Rayleigh scattering cross section has a sine function dependence on this angle, the arrangement provides optimum Rayleigh scattering signal when using both lines simultaneously. A quartz achromatic lens focuses the beam to form the probe volume. This lens is specifically designed for the second and fourth harmonics of the Nd:YAG laser and has the same focal length (400 mm) for both the green and the uv lines hence making the beam waist (probe volume) of the two lines coincident. The laser is operated at 10-Hz repetition rate, and under this condition, the conversion efficiency of the fourth harmonic generator is only about 14%. The pulse energies at the probe are measured to be 8.8 and 1.2 mJ for the 532- and 266-nm lines, respectively. However, because the Rayleigh scattering cross section for the uv line is 16 times that for the green, the Rayleigh signal from the uv line is still twice as strong. The laser beam is terminated inside a beam dump past the probe volume.

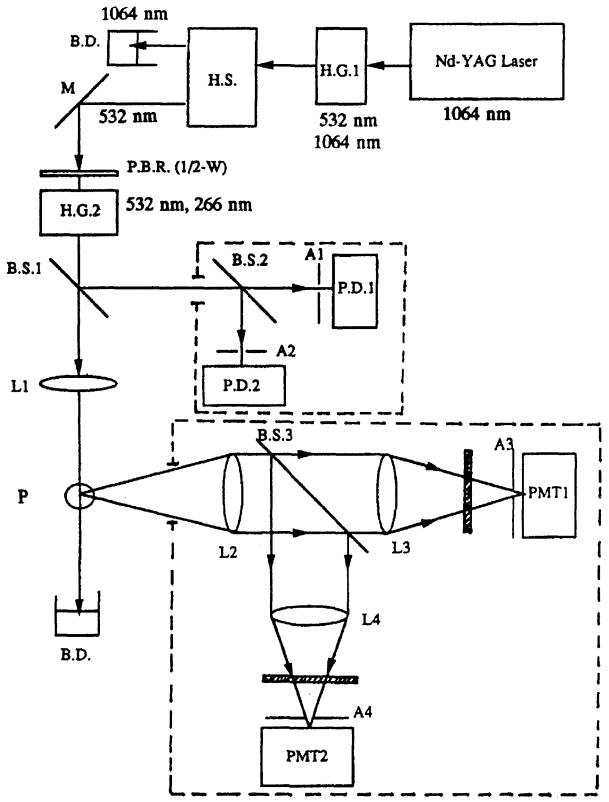

Fig. 1 Optical arrangement for the DLDR system: A, pinhole; B.D., beam dump; B.S., beam splitter; H.G., harmonic generator; H.S., harmonic separator; L, lens; M, mirror; P, probe; P.B.R., wave plate; P.D., photo diode; and PMT, photomultiplier tube.

The Rayleigh scattered light from the probe volume is collected by a 300-mm focal length quartz lens and at a 90 deg angle to the propagation direction of the beam. The collimated light is color separated using a dichroic splitter, and the signal from each line is sent to a separate photomultiplier tube (PMT). Before entering the pinhole and the PMT, each signal is passed through an interference filter at the appropriate wavelength to prevent signal cross talk and to discriminate against broadband background. To account for the pulse-to-pulse energy variation of the laser, the Rayleigh signal is normalized by the laser output at each shot of the laser. To accomplish this, a small portion of the laser beam is split just before the achromat that forms the probe volume (Fig. 1) and is subsequently

color separated using a second dichroic splitter. The laser light from each line is fed to a photodiode, the output of which is sampled along with those of the PMTs during each shot of the laser.

The PMT output of Rayleigh scattering signal and the laser reference output from the photodiodes are fed to sample-and-hold units and subsequently digitized by a 12-bit, 8-channel analog-to-digital converter. The digitized data are stored in a personal computer for postprocessing. Video amplifiers are used to optimize the individual outputs from the PMTs. Data are collected from all four channels at each pulse of the laser (10-Hz repetition rate), which is processed to yield local, time-frozen temperature or pressure. A trigger pulse, synchronized with the Q-switching of the laser, initiates the data sampling.

Results

System Calibration

The Rayleigh scattering system was calibrated several times under different sets of conditions. The temperature calibrations were undertaken using a hot air jet. The system was also calibrated against gas pressure using a vacuum chamber. In each case, the calibration procedure was repeated several times with various levels of laser line background in the collected signal to determine the value of the surface scattering ratio β and to assess the effect of background level on calibration accuracy.

The hot air jet has an inner core whose temperature can be controlled and a surrounding coflow that is kept at ambient temperature. The supply air to the jet is filtered in order to eliminate particulates in the flow, thus avoiding the contamination of the Rayleigh signal by Mie scattering. The laser probe is positioned at the centerline of the jet, approximately two inner jet diameters downstream from the exit plane. The jet temperature is measured by a thermistor, which is placed immediately downstream of the laser probe.

Figure 2 shows two representative calibration curves obtained using the jet whose temperature was varied between 290 and 780 K. Different levels of background noise were obtained by scattering some of the laser light from an aluminum plate placed within the line of sight of the collecting optics, on the opposite side of the probe volume. Each data point is an average of 1000 shots of the laser. The normalized Rayleigh signal grows linearly with inverse temperature while background due to laser glare adds a bias to the collected signal. Obviously, if not accounted for, this bias can cause large errors in temperature measurements. For both sets of calibrations, the scatter in the data is quite small; the relative standard deviation for Fig. 2a is 3.6, whereas this value is 4.6 in Fig. 2b. The effect of background contamination on the green line is more pronounced due to the smaller Rayleigh scattering cross section at this wavelength. The scattering cross section increases with shorter wavelengths resulting in higher signal energies in the uv and, thus, lower levels of relative background compared to the green line. The results of the air jet calibrations are summarized in Table 1. These results represent six individual calibrations similar to the two shown in Fig. 2, each with a different background level.

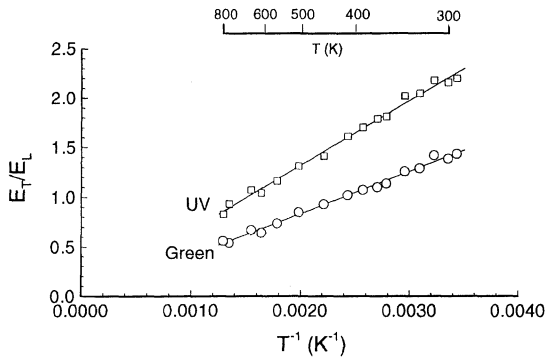

a) Without background contamination

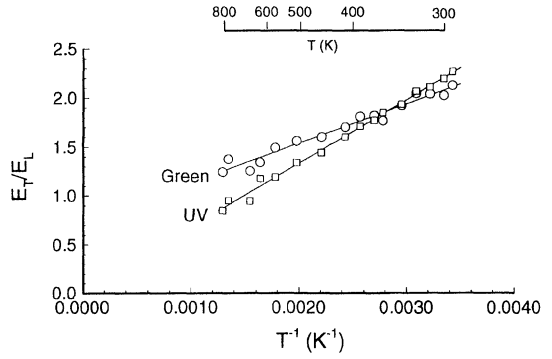

b) With background contamination

Fig. 2 Air jet calibrations.

Table 1 Summary of temperature calibrations, P = 760 torr

	C_1 ($\times 10^{-6}$), m-sr	C_2 ($\times 10^{-5}$), m-sr	β
Average value	1.365	1.354	2.15
Standard deviation	0.047	0.04	0.11
Percent deviation	3.44	2.95	5.1

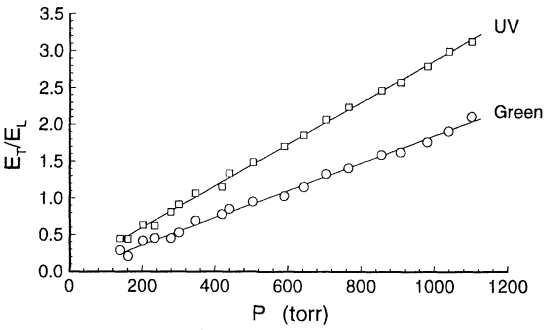

a) Without background contamination

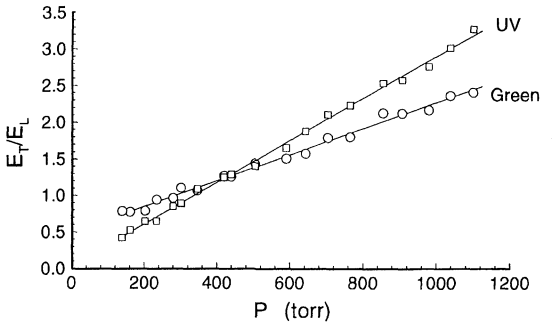

b) With background contamination

Fig. 3 Vacuum chamber calibrations.

The vacuum chamber used for the pressure calibrations is of the cross-hair type, consisting of two hollow orthogonal cylinders, which intersect at the center of the chamber. Quartz windows are placed at the ends of each cylinder. The laser beam travels through one cylinder forming the probe volume at the crossing of the two cylinders. The scattered light is collected through one window of the other cylinder. An aluminum plate is placed outside of the opposite window, which is used to scatter laser glare into the test chamber. When the plate is removed from the window, the Rayleigh signal is free of background noise. Figure 3 shows two representative calibrations: with no background noise present in the Rayleigh signal (Fig. 3a) and Rayleigh signal with some background contamination (Fig. 3b). Each data point on the graph represents an average of 1000 individual realizations. These pressure calibrations also show a linear dependence of signal on gas pressure with little scatter in the data. Again, the uv signal is much less sensitive to the background noise than the green line is. The results of six sets of pressure calibrations with varying levels of background noise are

Table 2 Summary of pressure calibrations, T = 298 K

	C_1 ($\times 10^{-6}$), m-sr	C_2 ($\times 10^{-5}$), m-sr	β
Average value	1.387	1.379	2.07
Standard deviation	0.051	0.044	0.1
Percent deviation	3.68	3.19	4.8

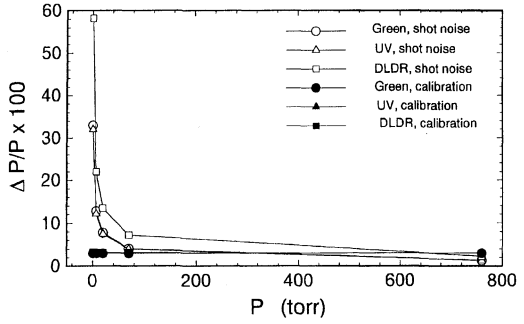

Fig. 4 Error estimates for vacuum pressure measurements.

summarized in Table 2. The calibration constants in Table 2 are very close to those obtained earlier through temperature calibrations and summarized in Table 1, indicating that both procedures can be used to obtain accurate calibrations. In both cases, the uncertainty due to random scatter in data is small giving further confidence in the optical system and the calibration procedures. Another important outcome of the calibrations is the value of β, which is approximately 2 in both calibrations. This indicates that surface scattering of the laser light in the uv line is only half as strong as in the 532-nm green line. Therefore, since the Rayleigh scattering cross section has λ^{-4} dependence on the wavelength, the signal-to-background noise ratio of the uv line is about 32 times larger than the green line.

Using the results in Tables 1 and 2, an analysis is carried out to assess the reliability of the optical system in the measurement of vacuum pressures. In single-shot measurements, the two primary sources of error are shot noise and the uncertainty in the calibration constants. For single-line detection, the relative error in pressure due to the uncertainty in C is given by

$$\frac{\Delta P}{P} = \left\{\left[\left(\frac{E_T}{E_L}\right)\left(\frac{1}{C^2}\right)\right]\Big/\left[\left(\frac{E_T}{E_L}\right)\left(\frac{1}{C}\right) - C'\right]\right\}\Delta C \qquad (5)$$

whereas for the dual-line operation, this error can be expressed as

$$\frac{\Delta P}{P} = \left(\left\{\left[\left(\frac{E_{T,1}}{E_{L,1}}\frac{1}{C_1^2}\right)^2(\Delta C_1)^2 + \left(\frac{E_{T,2}}{E_{L,2}}\frac{\beta}{C_2^2}\right)^2(\Delta C_2)^2\right]^{\frac{1}{2}}\right\}\Big/\left(\frac{E_{T,1}}{E_{L,1}}\frac{1}{C_1} + \frac{E_{T,2}}{E_{L,2}}\frac{\beta}{C_2}\right)\right) \qquad (6)$$

Because the background noise is determined explicitly and eliminated from the Rayleigh signal in DLDR technique, C' has no influence on the relative error in pressure and, hence, does not appear in Eq. (6). For the present system, the relative error in pressure becomes $\Delta P/P \approx 0.035$ in the absence of background noise. The error in pressure due to calibration uncertainty is shown in Fig. 4 along with that due to photon shot noise (for single-shot measurements). The background level is assumed to be zero for the single-line detection. The shot noise error is due to the uncertainty in the number of detected photons at each measurement and is calculated from Poisson statistics.[15] For single-line Rayleigh scattering measurements,

$$\frac{\Delta P}{P} = \left[\left(\frac{hc}{\lambda}E_T\right)^{\frac{1}{2}}\right]\Big/\left[\frac{E_T}{E_L}\frac{1}{C} - C'\right]CE_L \qquad (7)$$

For the DLDR method, the relative error in pressure due to shot noise is given by

$$\frac{\Delta P}{P} = \left\{\left[\left(\frac{kT}{E_{L,1}C_1(\sigma_1 - \beta\sigma_2)}\right)^2\left(\frac{hc}{\lambda_1}E_{T,1}\right) + \left(\frac{\beta kT}{E_{L,2}C_2(\sigma_1 - \beta\sigma_2)}\right)^2\left(\frac{hc}{\lambda_2}E_{T,2}\right)\right]^{\frac{1}{2}}\right\}\Big/\left[\left(\frac{E_{T,1}}{E_{L,1}}\frac{1}{C_1} - \frac{E_{T,2}}{E_{L,2}}\frac{\beta}{C_2}\right)\Big/\left(\frac{\sigma_1 - \beta\sigma_2}{kT}\right)\right] \qquad (8)$$

For the present optical system, the contribution of the calibration constant uncertainty to the overall measurement error is relatively small (≈3.5%) for both single-line and dual-line operation. On the other hand, the shot noise error has a strong dependence on gas pressure at low pressures. This is due to the fact that the Rayleigh scattered energy decreases with decreasing gas pressures, which in turn increases the relative shot noise. It is also noted that measurement error due to shot noise is larger for the dual-line detection method as compared to the single-line operation. The laser used for the present study has a relatively low-pulse energy (approximately 10 mJ) compared to the new generation Nd:YAG lasers, which can produce pulse energies of the order of a joule. Even then, the shot noise uncertainty of the present DLDR system is significantly improved over the previous copper-vapor laser-based system.[15] For example, at 760 torr, the relative uncertainty of the present DLDR system is calculated to be 2%, whereas this number for the copper-vapor based system is about 5%. At a vacuum pressure of 20 torr, these levels become 13 and 35% for the Nd:YAG- and copper-vapor-based systems, respectively. Clearly, at this pressure, it is not possible to obtain reliable single-shot measurements using the latter system.

Pressure Measurements

Figure 5 compares pressures measured by the DLDR system to those obtained using a gauge in the vacuum chamber. Pressure measurements were obtained at each shot of the laser, and each data point correspond to the average of 1000 such pressure realizations. The agreement between the two sets of measurements is strong although most of the Rayleigh data fall slightly below the straight line, which represents a perfect agreement between these measurements and those from the vacuum gauge, indicating that the DLDR measurements slightly underestimate the pressure. The rms of the 1000 individual pressure realizations are shown as solid-line error bars. These measured uncertainties are slightly larger than those estimated using Eq. (8), which are shown as dashed bars. Electronic noise also contributes to the measurement uncertainty in addition to the shot noise, thus leading to slightly larger uncertainties than those estimated.

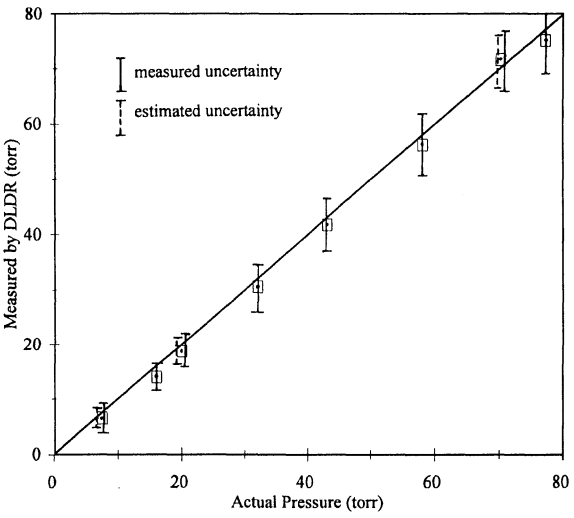

Fig. 5 Vacuum pressure measurements using DLDR system.

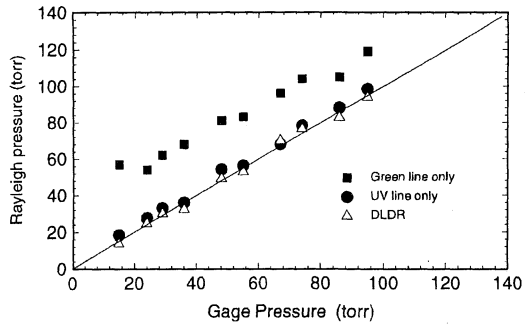

Fig. 6 Comparison of single-line and DLDR measurements of pressure.

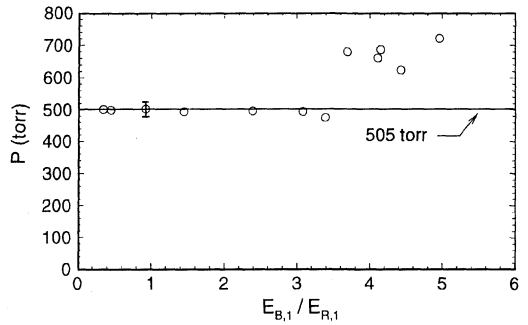

Fig. 7 Effect of background level on DLDR pressure measurements.

Pressures obtained using the DLDR method are compared to those from single-line detection Rayleigh scattering in Fig. 6. The Rayleigh scattered signal is intentionally contaminated by surface scattered background noise. The results closest to those of the vacuum gauge are obtained by the DLDR method. The uv single-line detection results are also close to those of the vacuum gauge, although they are slightly but consistently larger due to the background contamination. The single-line detection using the 532-nm green line gives, by far, the poorest results. The background noise nearly overwhelms the Rayleigh signal in the green line although its effect on the uv signal is still small. Therefore, for single-line operation, the uv line should be the choice for better signal-to-background noise characteristics, although if measurements with the highest possible level of accuracy are needed, the dual-line detection technique is preferable.

Figure 7 shows pressure results obtained by the DLDR system under different levels of background. These measurements were made in order to determine the maximum level of background noise-to-Rayleigh signal ratio under which reliable gas pressures can be obtained. These measurements were made at a fixed cell pressure of 505 torr (measured by the vacuum gauge) and under several background levels. The air temperature in the chamber was kept at 298 K. Under these conditions, the average Rayleigh scattered signal is constant while the background contamination level is varied. In Fig. 7, the signal-to-noise levels are based on the 532-nm green line. The Rayleigh scattered energy $E_{R,1}$ is calculated using gas pressure measured by the vacuum gauge while the background is determined from the DLDR measurements [Eq. (4)]. Again, each data point represents an average of 1000 pressure realizations obtained at each shot of the laser. The figure indicates that accurate pressure measurements are possible even when the background noise-to-Rayleigh signal ratio is as high as three. For ratios $E_{B,1}/E_{R,1} > 3$, the system overestimates the gas pressure, most likely due to the saturation of the photomultiplier tube for the green line at this light level. The corresponding background-to-signal ratio in the 266-nm line is still significantly smaller ($E_{B,2}/E_{R,2} \approx 0.1$) since the signal-to-noise characteristics of the uv line are 32 times better that of the green, as pointed out earlier. Therefore, under the same background conditions, if only the uv line were to be used for detection, instead of the dual-line method, the pressure would be overestimated by approximately 10%.

Temperature Measurements

The temperature measurements were made in the heated air jet described earlier. Instantaneous temperatures were obtained at each shot of the laser in the initial development region of the heated jet in the presence of different levels of background laser glare. From long records of these instantaneous temperatures, radial and axial distributions of mean and turbulent temperature were obtained. These results are compared to those obtained using single-line Rayleigh scattering measurements, as well as to those from a fast-response thermistor. Figure 8 shows the mean temperature distribution across the coflowing jet 7 diameters downstream of the exit. In the Rayleigh scattering measurements, the signal is intentionally contaminated by laser glare to test the optical results. The same method as in the jet calibrations is used for background contamination. The record length for each data point is 3000 in both the Rayleigh scattering and the thermistor results. Figure 8 indicates that the thermal jet goes through a rapid initial development; the temperature profile at $x/d = 7$ has a nearly Gaussian profile, which is a characteristic of the self-preserving jet. The DLDR results agree very well with those of the thermistor whereas both the uv and the green line only results underestimate the jet temperatures due to the background noise. However, whereas the 532-nm single-line errors are unacceptably large for any practical application, the errors in the 266-nm single-line detection are relatively small.

The turbulent temperature profile obtained by the DLDR system at $x/d = 7$ is shown in Fig. 9 along with the corresponding thermistor result. The two measurements are in good agreement although, on the average, the DLDR measurements give slightly higher results than those of the thermistor. This is partially due to the effect of shot noise, which tends to increase rms of temperature. The turbulent temperature profile agrees well, both quantitatively and qualitatively, with previous results of heated air jets with the

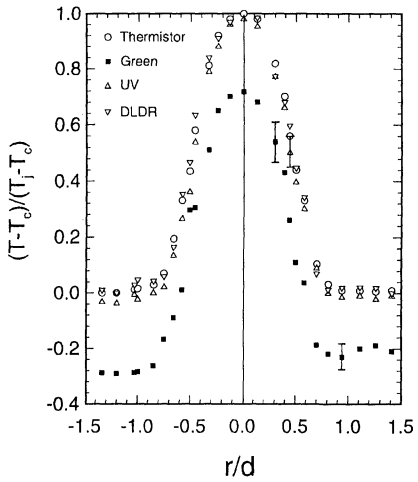

Fig. 8 Mean temperature profiles in heated jet, x/d = 7.

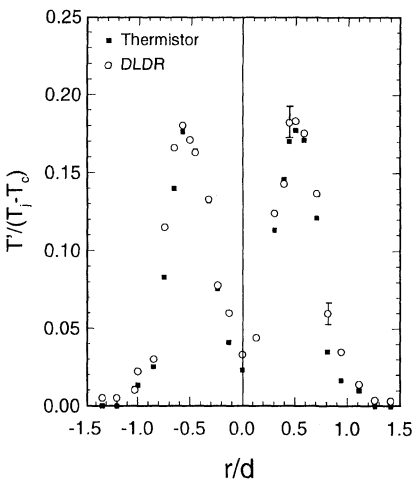

Fig. 9 Turbulent temperature profiles in heated jet, x/d = 7.

maximum intensities located around maximum mean temperature gradients.

Conclusions

In single-shot measurements, the calculated shot noise uncertainty in the pressure is higher for the DLDR technique compared to single-line detection. However, single-shot measurement uncertainties of the present system are much better than those of the previous copper-vapor laser-based system. In the presence of high levels of background, the best and the worst measurement accuracies are obtained by the DLDR and green line only systems, respectively. The uv line only results are relatively close to those of the DLDR technique. This is due to the fact that the uv Rayleigh scattering cross section is 16 times larger, whereas the surface scattering is only half that of green, as determined from system calibrations. The combined effect is that the uv signal-to-background noise ratio is over 30 times larger than that of the green. Therefore, using the uv line only is in itself an improvement over using the green line alone. Further pressure tests showed that the DLDR technique works robustly up to a level where the background-to-signal level on the green line is approximately 3. At this level of background contamination, the uv background-to-signal ratio is about 0.1. Therefore, the DLDR method still provides a significant improvement over uv only measurements. Single-shot temperature measurements were made in an axisymmetric heated air jet using both the single-line detection and the DLDR methods. The mean and turbulent temperature profiles obtained 7 diameters from the jet exit are in excellent agreement with those of a fast response thermistor.

Acknowledgments

Support through NASA Grant NAG-3-1301, with R. G. Seasholtz as the Technical Monitor, is gratefully acknowledged.

References

[1]Bill, R. G., Jr., Namer, I., Talbot, L., and Robben, F., "Density Fluctuations of Flame in Grid Induced Turbulence," *Combustion and Flame*, Vol. 44, No. 2, 1982, pp. 277–285.

[2]Gouldin, F. C., and Halthorne, R. N., "Rayleigh Scattering for Density Measurements in Premixed Flames," *Experiments in Fluids*, Vol. 4, No. 3, 1986, pp. 269–278.

[3]Dibble, R. W., and Hollenbach, R. H., "Laser Rayleigh Thermometry in Turbulent Flows," *Proceedings of the 18th Symposium on Combustion*, Combustion Inst., Pittsburgh, PA, 1981, pp. 1489–1499.

[4]Namer, I., and Schefer, R. W., "Error Estimates for Rayleigh Scattering Density and Temperature Measurements," *Experiments in Fluids*, Vol. 3, No. 1, 1985, pp. 1–9.

[5]Graham, S. C., Grant, A. J., and Jones, J. M., "Transient Molecular Concentration Measurements in Turbulent Jets," *AIAA Journal*, Vol. 12, No. 8, 1974, pp. 1140–1142.

[6]Dyer, T. M., "Rayleigh Scattering Measurements of Time-Resolved Concentration in a Turbulent Propane Jet," *AIAA Journal*, Vol. 17, No. 8, 1979, pp. 912–914.

[7]Pitts, W. M., and Kashiwagi, T., "The Application of Laser-Induced Rayleigh Scattering to the Study of Turbulence Mixing," *Journal of Fluid Mechanics*, Vol. 141, April 1984, pp. 391–429.

[8]Arcoumanis, C., "A Laser Rayleigh Scattering System for Scalar Transport Studies," *Experiments in Fluids*, Vol. 3, No. 2, 1985, pp. 103–108.

[9]Ötügen, M. V., and Namer, I., "Rayleigh Scattering Temperature Measurements in a Plane Turbulent Air Jet," *Experiments in Fluids*, Vol. 6, No. 7, 1988, pp. 461–466.

[10]Miles, R., and Lempert, W., "Two-Dimensional Measurement of Density, Velocity, and Temperature in Turbulent High-Speed Air Flows by UV Rayleigh Scattering," *Applied Physics*, Vol. B15, No. 1, 1990, pp. 1–7.

[11]Miles, R. B., Lempert, W. R., and Forkey, J., "Instantaneous Velocity Fields and Background Suppression by Filtered Rayleigh Scattering," AIAA Paper 91-0357, Jan. 1991.

[12]Seasholtz, R. G., and Zupank, F. J., "Spectrally Resolved Rayleigh Scattering Diagnostics for Hydrogen-Oxygen Rocket Plume," *Journal of Propulsion and Power*, Vol. 8, No. 5, 1992, pp. 935–942.

[13]Elliot, G. S., Samimy, M., and Arnette, S. A., "Details of a Molecular Filter-Based Velocimetry Technique," AIAA Paper 94-0490, Jan. 1990.

[14]Kouros, H., and Seasholtz, R. G., "Fabry-Perot Interferometer Measurements of Static Temperature and Velocity for ASTOVL Model Tests," *Proceedings of the Symposium on Laser Anemometry: Advances and Applications*, edited by T. T. Huang and M. V. Ötügen, ASME FED-Vol. 191, American Society of Mechanical Engineers, New York, 1994.

[15]Ötügen, M. V., Annen, K. D., and Seasholtz, R. G., "Gas Temperature Measurements Using a Dual-Line Detection Rayleigh Scattering Technique," *AIAA Journal*, Vol. 31, No. 11, 1993, pp. 2098–2104.

G. Laufer
Associate Editor